

Color topographical map segmentation Algorithm based on linear element features

Tiange Liu · Qiguang Miao · Pengfei Xu ·
Jianfeng Song · Yining Quan

Received: 13 March 2014 / Revised: 29 January 2015 / Accepted: 13 February 2015 /
Published online: 24 February 2015
© Springer Science+Business Media New York 2015

Abstract In order to overcome the discontinuity of geographic elements during the digitization of scanned topographic maps, a color map segmentation algorithm, which is used to segment color maps into different layers based on linear element features, is proposed in this paper. Linear elements are regarded as the elementary units in this method. We use background removal, thinning, nodes disconnection, labeling and dilation to get the elementary units. Then the main color, which could accurately represent the color feature of linear element, is extracted for clustering on the basis of Fuzzy c-means algorithm. At last, disconnected nodes are merged into the corresponding layers to keep the continuity of the results. The experimental results show that the proposed algorithm outperforms other segmentation approaches that regarding pixels as the elementary units.

Keywords Color map segmentation · Linear element · Color features · Fuzzy c-means (FCM)

1 Introduction

Scanned topographic map digitization is widely used in geographic information system of transportation, tourism and military. In the case of that all geographic elements are mixed together in one scanned color map, the basis of digitization is classifying geographic elements, such as contour lines, roads and point-symbols, into different layers [25]. Most topographic maps use colors to help the user to distinguish different feature categories [12, 16, 28].

T. Liu · Q. Miao (✉) · P. Xu · J. Song · Y. Quan
School of Computer Science and Technology, Xidian University, Xi'an 710071 Shaanxi, China
e-mail: qgmiao@126.com

T. Liu
e-mail: xidianltg@126.com

P. Xu
e-mail: xpf1987071500@126.com

J. Song
e-mail: jfsong@mail.xidian.edu.cn

Y. Quan
e-mail: ynquan@mail.xidian.edu.cn

Therefore, classifying geographic elements into different layers is also defined as color segmentation in a color map. Figure 1 shows the expected result of color map segmentation. It can be seen that four color layers are separated from the original color map. Each layer represents one or a type of geographic elements, such as road and point-symbol layer, contour line layer, vegetation layer and river layer.

In recent years, many algorithms have been proposed for color topographic maps segmentation. Khotanzad and Chen employed color key set to comprehend color aliasing and false colors in maps thus to segment the color topographic maps [7, 12]. This method suffers from limited applicability to poor conditioned maps. Zheng et al. presented a color image segmentation method based on fuzzy clustering with two-dimensional histogram [30]. This unsupervised method can segment color map images automatically. However, it cannot overcome the problems of false colors and mixed colors due to the less consideration about the spatial relationship. In order to make full use of the information in color space, local homogeneity and connected regions of color layers, Leyk proposed a segmentation method based on Seeded Region Growing (SRG) and information of the local image, the frequency domain and the color space [15, 16]. However, this method still cannot overcome the disadvantage in the initial seeds selection and the order dependencies of SRG. It also requires extensive parameters, which leads to lacking of robustness.

In addition, there has been a remarkable growth of techniques for the segmentation of images. Segmentation based on histogram threshold is widely used in gray or color images [5, 14, 20, 22] for its high efficiency and simplicity. But these kinds of methods are lack of accuracy and they are difficult to be applied in inferior quality images. The Fuzzy c-means (FCM) algorithm gets a lot of popularity in image segmentation thanks to the successful introduction of fuzzification to every pixel. Compared with hard cluster methods, FCM algorithm could retain more original information of image [24]. Lim [18] and Blosca [2] adopted FCM to assign the unclassified pixels to the closest class at the coarse stage using the detected cluster centers in order to solve the problem of cluster validity with the coarse-fine

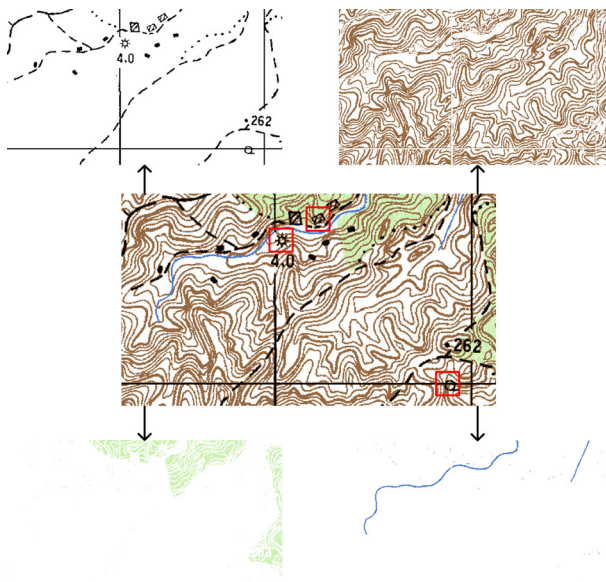


Fig. 1 The purpose of color image segmentation to color map

theory. Mohamed [1] presented a new algorithm named Bias-Corrected FCM (BCFCM), which modified the objective function of FCM to compensate for the gray (intensity) inhomogeneity and to allow the labeling of a pixel to be influenced by the labels in its immediate neighborhood. Moreover, by incorporating local spatial and gray information together, a novel fast and robust FCM framework for image segmentation called Fast Generalized Fuzzy c-means clustering algorithms (FGFCM) is proposed in [3]. In addition, artificial neural networks are also widely applied in image segmentation, such as Hopfield neural networks (HNN) [4, 11], self-organizing map (SOM) neural networks [21] and pulse-coupled neural network (PCNN) [13, 23, 26, 31].

Here, we present a color map segmentation method which employs the linear elements as elementary units. This method could significantly improve the completeness and correctness of segmentation results compared with the existing algorithms. There are three advantages which make the good performance of this method possible. Firstly, the background removal method applied could accurately extract linear elements, i.e. the fundament of segmentation is highly strong. Secondly, the linear elements and their features used in segmentation could represent the geographic elements appropriately, which make the segmentation effectively. Lastly, the merging of disconnected nodes after segmentation could further improve the completeness of segmentation results.

This paper is organized as follows: analysis about the shortages of existent methods and the difficulties in color map segmentation are given in section 2. In section 3, the proposed method is described in detail. Some objective evaluation metrics are introduced in section 4. Experiments which indicate the superiority and effectiveness of our proposed method are implemented and analyzed in Section 5. Finally, the concluding remarks are given in section 6.

2 Analysis

In general, the existing color map segmentation methods can be classified into two types. One is based on the color features of pixels, which regards a single pixel as an elementary unit in the segmentation process [7, 12, 30]. These methods distinguish pixels on the basis of similarity in color between pixels and centers of prototypes, which result in their high efficiency and easy to be achieved. Since lacking of space features, they are not robust to deal with noisy points. The other one considers both color features and local features of the image [1, 3, 15, 16] and it can overcome the noise problem to some extent. However, the shape of neighbor regions always are circles or rectangles and are not direction-oriented, which limits its application in confronting mixed and false colors. If using these methods mentioned above, some pixels in line features could be falsely segmented into other layers which will lead to the fracture of linear elements. These results were caused by the serious false colors and color aliasing which are influenced by different kinds of factors during the process of map-making and scanning. False colors are caused by RGB misalignment in the scanner. RGB misalignment occurs whenever the red, green, and blue color planes are not perfectly registered. Physical and optical misalignments are the two major causes of RGB misalignment [12]. For instance, as shown in Fig. 2a, the original color of contour lines should be brown. However, it can be seen that, affected by RGB misalignment, the color of some pixels are converted to green and purple after scanned. This would cause the incompleteness and fracture of the linear elements. On the other hand, aliasing is induced by the scanner's point spread function. Color deviation shown in Fig. 2b is caused by overlap of contour line and vegetation. For the aliasing and mixing, pixels in overlapping colors will lose their original color features [12]. In Fig. 2b, the zoomed-in pictures show normal contour line and overlapping contour line

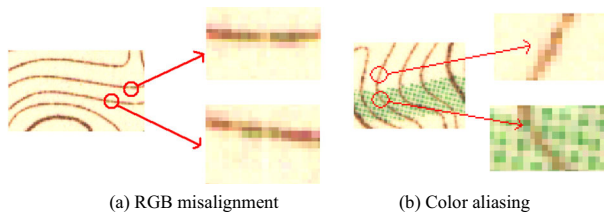


Fig. 2 Color deviation in a map

respectively. It can be seen that pixels on the overlapping contour line have deviations in color. Figures 2, 5, 7 and 9 are parts of a scanned color topographic map whose horizontal resolution and vertical resolution are both 96. The scanning resolution is a key technical parameter in determining the quality of images. High resolution images could keep details in it which will reduce color deviation. Unfortunately, lots of maps are not scanned in sufficient high resolution, just as the images mentioned above. In this case, the width of most lines is only two or three pixels, which makes color deviation occupies a large portion in pixels of lines. Thus, the color image segmentation in low scanning resolution maps is still a big challenge.

Three types of elements, line (such as contour line and road), point (such as point-symbol) and area (such as vegetation), are contained in a topographic map (as shown in Fig. 1). Point features in maps are always drawn as closed or not closed curves which correspond to their geographic elements, like symbols marked by red rectangle. In addition, both point features and line features will be kept after removing the areal elements. So, two definitions are given as following.

- **Linear elements** are defined as the closed/not closed curves which include points and lines in maps. And the linear element features represent the characteristics of linear elements such as color features, shape features and textural features.
- **Areal elements** are the background and area (such as vegetation) in maps.

Hence, all pixels in a map can be classified as either linear elements or areal elements. As we all know, most information in a topographic map is expressed by linear elements, thus they play a vital role during the process of color map digitization. Meanwhile, areal elements can only provide the information through their boundary, which means most pixels in areal elements are insignificant. What is more, the areal elements in a color map are often blurred and contain mixed colors for its improper preservation or the influences of external factors when scanned. Consequently, the results of segmentation are easily affected by these factors.

Hong Chen [6] proposed a color map segmentation method based on object-oriented technology. Compared with other color map segmentation methods, it not only combines color feature and spatial feature, but also breaks through the size limitation and non-direction of neighbor regions, by regarding connected region as the elementary units. Firstly, the linear elements are separated from the areal elements using a simple threshold method based on RGB color feature for image segmentation. Then the line features are thinned and the nodes are disconnected. Finally, these independent one-pixel width linear elements are segmented into different layers by using the average color value as their color features. The continuity of linear elements can be preserved to some extent and the result obtained is relatively ideal. However, there still are some defects: (1) the method for removing the areal elements is oversimplified because the threshold method for image segmentation is more suitable for the maps in high quality to separate areal elements from linear elements rather than for those which are blurred.

(2) The linear elements are located in the centre line of original linear elements after been thinned. But for the linear elements which are blurred or mixed with the areal elements, there still exist large amounts of mixed colors in the centre line. Thus, the proportion of mixed colors will increase with the reduction of pixels in the linear elements. Even a few mixed color pixels would occupy a large proportion in a thinned linear element. (3) Color features of the linear elements cannot be accurately represented because average color value could be interfered by the mixed colors. (4) Since the disconnected nodes are not merged into layers after segmentation, it will cause information losing and poor continuity of linear elements.

Considering these problems, we propose a new color map segmentation method based on linear element features. The elementary unit used for segmentation is not single pixel but linear elements. Firstly, the background removal algorithm base on energy density and shear transform is used to remove the background and the areal elements [19]. Secondly, thinning, nodes disconnection, labeling and dilation, are employed to process the linear elements successively. The linear elements are separated by FCM based on the main color features previously calculated. Lastly, the linear elements of each layer are thinned and the disconnected nodes are merged into the corresponding layers so that the linear elements can be more continuous. The new method can discover the distribution of linear geographic elements from the background removed results. This prior knowledge in distribution of linear elements plays an important guiding role in the later segmentation. This method not only regards the linear elements as unit which could guarantee the continuity in results, but also employs the main color as the feature of each linear element which could overcome the problems of noise, false color and color aliasing. This region based segmentation method which has a prior knowledge in region partition, could significantly improve the accuracy of segmentation results. In addition, the merging of disconnected nodes could further improve the completeness of the obtained results.

3 Color map segmentation method based on linear element features

3.1 Overview of the method

In this section, a new algorithm named Color Map Segmentation method based on Linear Element Features (CMSLEF) and the specific steps are introduced. The input of this method is an original scanned topographic map. After the processes of areal elements removal, thinning, nodes disconnecting, dilating and clustered by FCM, the results are obtained by merging the disconnected nodes to the layers obtained by classification. The flow chart of CMSLEF is shown in Fig. 3.

3.2 The areal elements removal method

The areal elements removal method proposed by Miao etc. [19], which is based on energy density and the shear transform, is adopted in our method. This method proposed a concept of energy density, which can reflect the degree of the energy concentration in a grayscale image, is defined as the average energy of a region. It is described by the following formula.

$$E = \frac{1}{M \times N} \sum_{i=1}^M \sum_{j=1}^N f(i, j)^2 \quad (1)$$

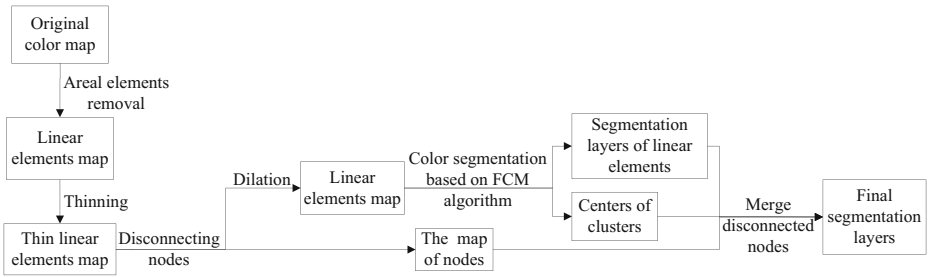


Fig. 3 The flow chart of CMSLEF

where E is the energy density, $M \times N$ is the size of the area, $f(i, j)$ is the gray-level of a pixel in the grayscale image. Then two templates, both in vertical direction and horizontal direction, for linear separation from background are built. The energy density of lines and background can be calculated with these templates, then linear features and background can be separated from each other based on the difference of the energy densities.

Furthermore, in order to solve the problem that linear features may be lost in the process of linear separation due to the directional limitation (some lines can only be separated in one direction), the shear transform [17] is applied to get n directions of affine images. The shear transform is an affine transforms which is a very convenient tool to provide directionality in the sense that it preserves important geometric information such as length, angles, and parallelism. We had detailed the shear transform in our previous work [19], which will not be explained in this method. In our method, the number of directions n is usually equal to 3 which corresponding to 0° , -45° and 45° . That is because in a small region on grid image, these three directions could contain almost all trends of lines. The flow diagram of this method is shown in Fig. 4.

In this method, a threshold T of the energy density difference between the linear elements and areal elements needs to be set to extract linear elements from the original color map. An overlarge value for T which would make it difficult to separate the linear element (some of them may be wrongly recognized as areal element) could cause the incompleteness of results for the linear element extraction. Similarly, an undersized value for T which would pose a

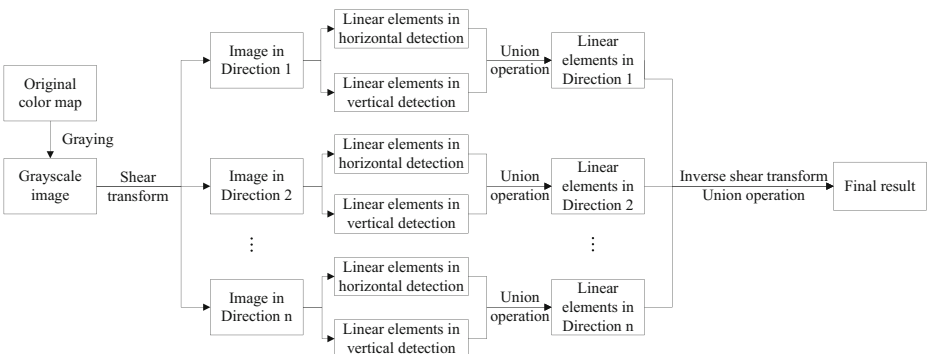


Fig. 4 The flow diagrams of areal elements removal method

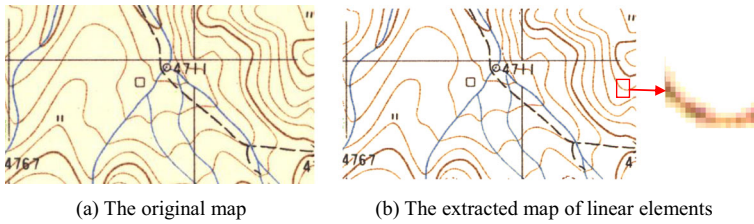


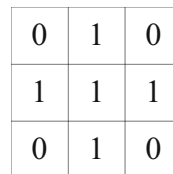
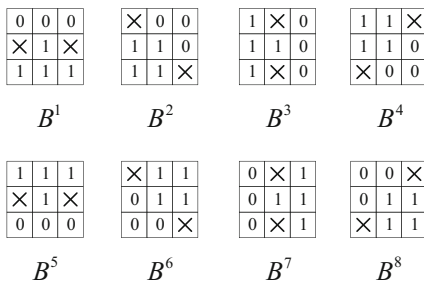
Fig. 5 The result of background removal

challenge on removing the areal element (some of them probably be judged as linear element and maintained) could result in the incorrect information is included in the final extraction result. Figure 5 shows the original map and the linear elements map after background removal. It can be seen that all the background color disappears in Fig. 5b. Meanwhile, lots of false colors, as shown in the zoomed-in inset, are kept which guarantee the continuity of contour line. What’s more, Fig. 7 shows the contour lines after areal element removal, which overlap with vegetation in original map. The zoomed-in image indicates numerous aliasing and mixed colors are retained in contour lines which also guarantee the continuity of contour line. In this way, the process retains the linear elements, avoiding the interruption caused by false color and color deviation as well.

3.3 Methods for thinning and dilation of linear elements

Thinning algorithm reduces the line width from multi pixels to one pixel in the binary image. The thinning algorithm based on the classical mathematical morphology [8], using the group of structure elements shown in Fig. 6a, is employed to thin the linear elements and a thinned linear element map (Fig. 9c) is obtained. The purpose of thinning is to find the intersections of the linear elements. Pixels with more than two neighbors are regarded as nodes which need to be separated from thinned linear element map. After this disconnecting process, nodes map (Fig. 9d) and disconnected thinned linear element map (Fig. 9e) are achieved.

Although the linear element after thinning can maintain the continuity, one-pixel-width linear element will lose the majority of the color information of the linear elements. Furthermore, the color features of thinned linear elements cannot represent



(a) The group of structure elements for thinning (b) The expansion operator

Fig. 6 Operators for mathematical morphology operation. The symbol ‘×’ means without consideration

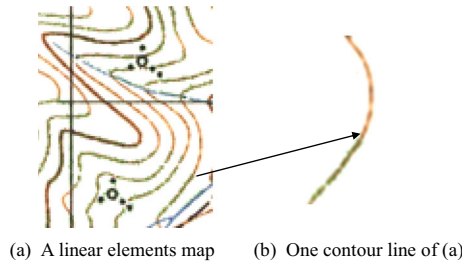


Fig. 7 A type of linear elements in color map

the original linear element features well if there are too much mixed colors contained in the thinned linear elements. Therefore, as the great supplement of the thinned linear elements, it is necessary to obtain the corresponding pixels and their neighbor pixels from the original linear element map, which is shown in Fig. 9b as an example. The dilation algorithm based on morphological dilation [8] with the expansion operator shown in Fig. 6b is employed in expanding the thinned linear elements in order to get the corresponding region of the original pixels. Specifically, the new pixels added by dilation have to be certainly obtained from the original linear map. So, if there are no pixels in the original linear map corresponding to these new added pixels, the new pixels should be removed from the dilated map (Fig. 9f).

3.4 Extraction of linear element color features

Color, as the foundation of distinguishing geographic elements, is the most important information in color map segmentation. Thus, the accuracy of the element color features has a great effect on the result of segmentation. Chen [6] uses the average color value as the linear element color feature. Although it is easy to achieve, average color value cannot precisely represent the color feature of linear element when mixed colors exist. A type of linear elements in color map is shown in Fig. 7. Figure 7a is a map of linear elements and a contour line in it is shown as Fig. 7b. There are lots of green pixels mixed in the contour line, which is caused by overlapping of contour line and vegetation. Obviously, it is inaccurate to regard average color value as color feature.

Therefore, we define the majority color of pixels as the main color to represent the linear element feature. In this way, if there are several main colors in one linear element, the average color should be calculated first, and the one which is the nearest to the average color would be chosen as the main color.

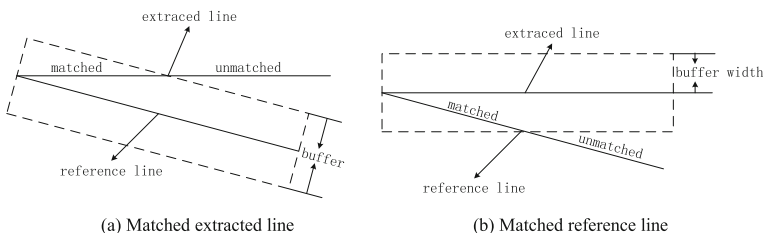


Fig. 8 Matching principle

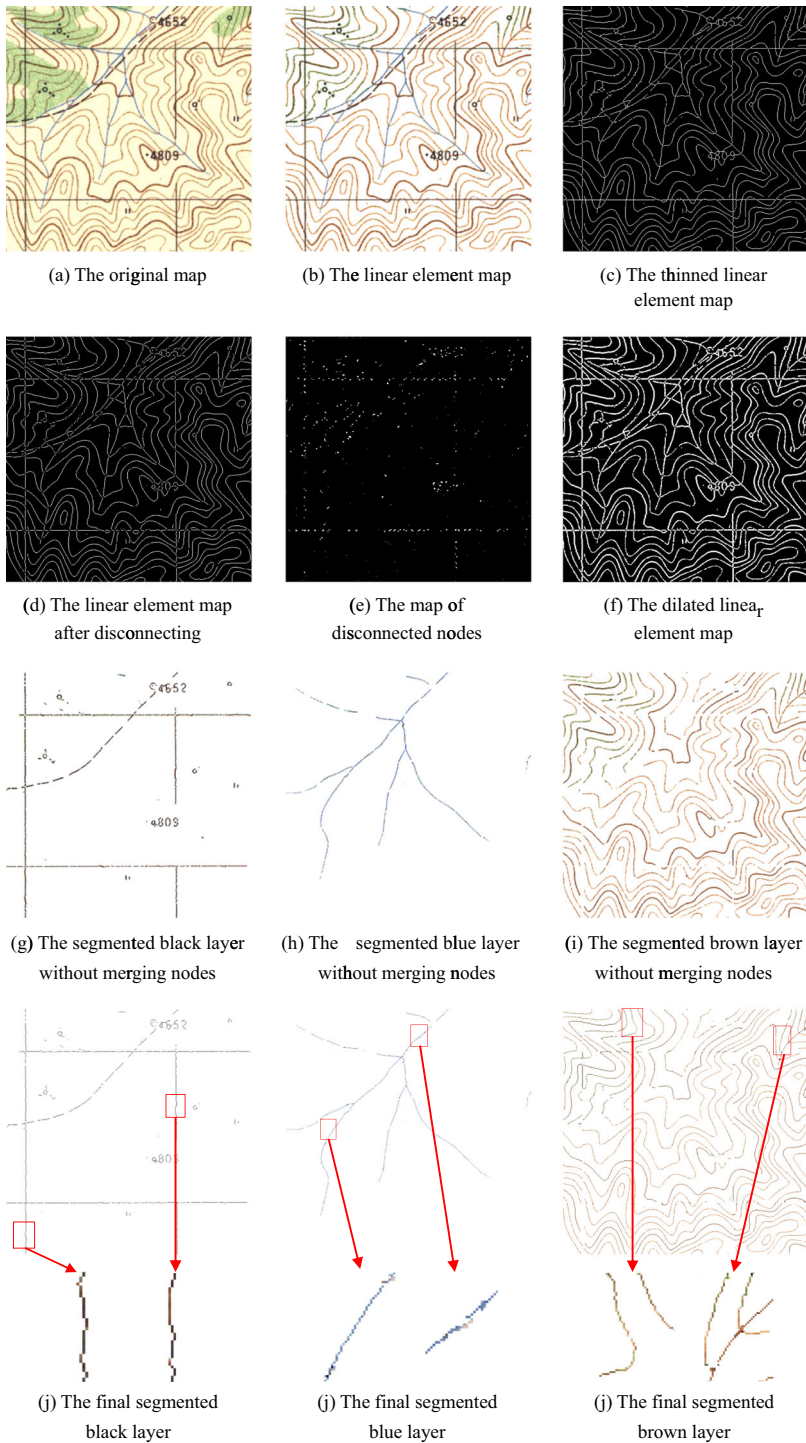
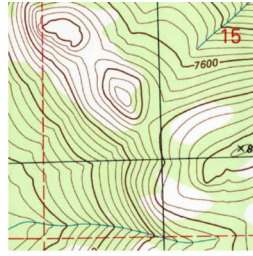
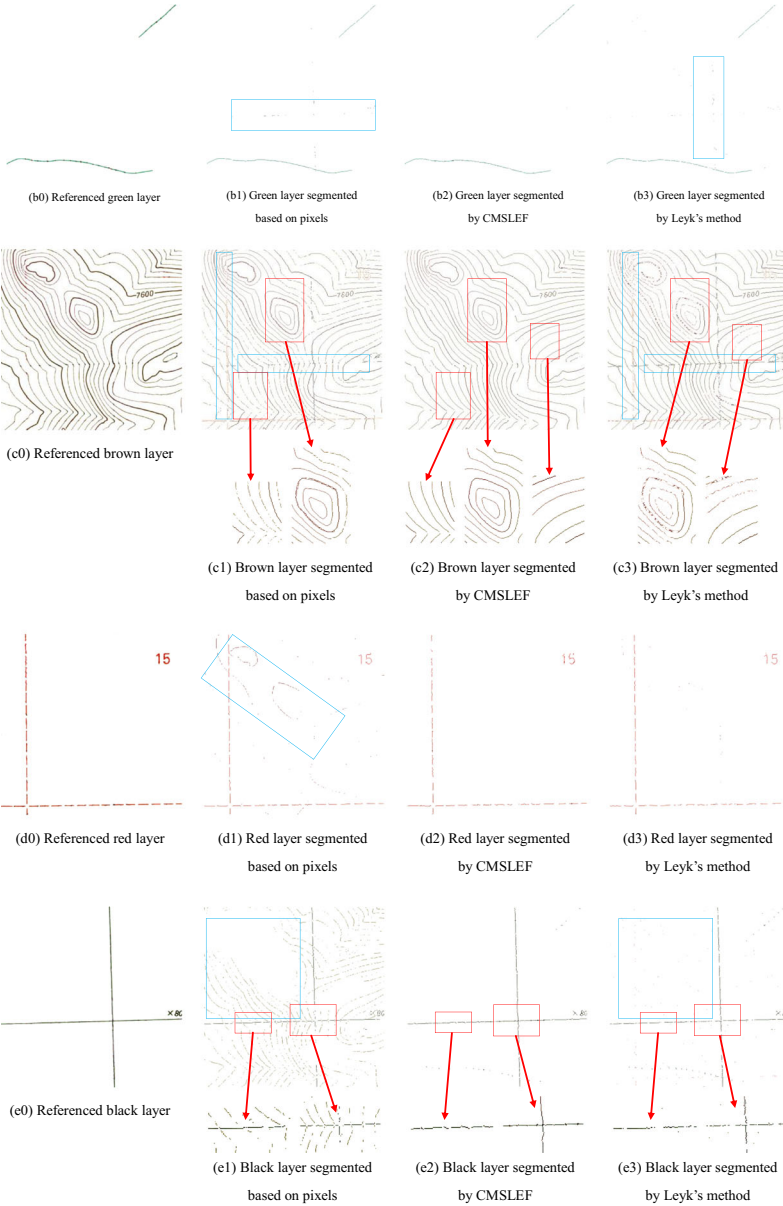


Fig. 9 The results of each experimental procedure



(a) An original map



◀ **Fig. 10** Results of comparison experiment. The red rectangles show superiority of our method in connectivity and the blue rectangles indicate fewer interferential pixels in results of CMSLEF. For Leyk’s method, we set $h_{crit}=0.95$, $d_{crit}=40$ and $c_{crit}=50$

3.5 Segmentation

We employed FCM algorithm to segment independent linear elements into different layers. Assume that $X=(x_1, x_2, \dots, x_n)$ is the set of linear element features with the purpose of c partitions. Let $V=(v_1, v_2, \dots, v_c)$ represents a c -tuple centers of clusters and $U=(u_{jk})_{c \times n}$ is a fuzzy membership matrix with u_{jk} denoting the grade of membership of feature point x_k in cluster j . The object function of FCM algorithm can be described as formula (1).

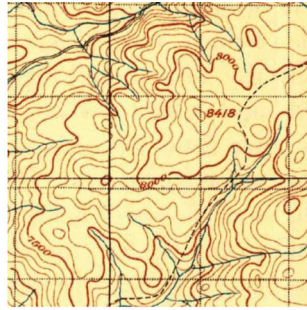
$$\min J = \sum_{k=1}^n \sum_{j=1}^c u_{jk}^m \|x_k - v_j\|^2 \tag{1}$$

where m is the weighting exponent on each fuzzy membership. A smaller m indicates a less fuzzier U , while a larger one indicates a fuzzier U . The choice of $m=2$ is widely accepted as a good choice [9, 29]. The fuzzy membership matrix U ($u_{jk} \in [0, 1]$) can be randomly initialized. The solution of formula (1) can be obtained through an iterative computation of formulas (2) and (3) until the object function converges to a stable state.

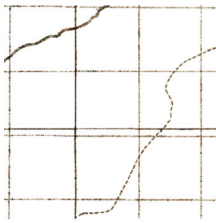
$$u_{jk} = \frac{\|x_k - v_j\|^{\frac{2}{1-m}}}{\sum_{i=1}^c \|x_k - v_i\|^{\frac{2}{1-m}}}, \quad k = 1, 2, \dots, n; j = 1, 2, \dots, c \tag{2}$$

$$v_j = \frac{\sum_{k=1}^n u_{jk}^m x_k}{\sum_{k=1}^n u_{jk}^m}, \quad j = 1, 2, \dots, c \tag{3}$$

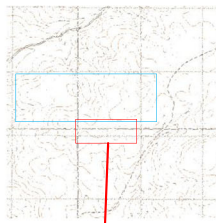
Then, each linear element is classified into the layer which corresponds to the largest $u_{jk}(k=1, 2, \dots, n)$ (Fig. 9g-i). In addition, the separated node pixels in section 3.3 are merged into their most similar layers based on the distance between them and the cluster centers $v_j(j=1, 2, \dots, c)$ in color space. Automatic vectorization of topographic map is mainly applied to trace pixels in each layer since one-pixel width results are more convenient for vectorization. Thus, before merging the nodes, thinning algorithm introduced in section 3.3 is applied to the segmented linear elements. Eventually, the final segmented layers are obtained (Fig. 9 j-l).



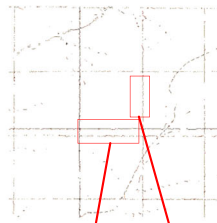
(a) An original map



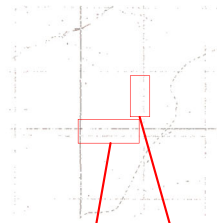
(b0) Referenced black layer



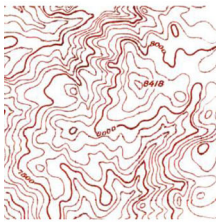
(b1) Black layer segmented based on pixels



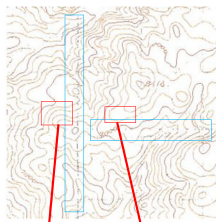
(b2) Black layer segmented by CMSLEF



(b3) Black layer segmented by Leyk's method



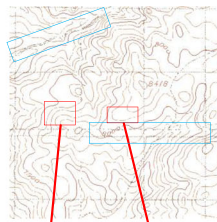
(c0) Referenced brown layer



(c1) Brown layer segmented based on pixels



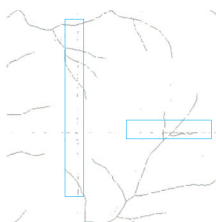
(c2) Brown layer segmented by CMSLEF



(c3) Brown layer segmented by Leyk's method



(d0) Referenced blue layer



(d1) Blue layer segmented based on pixels



(d2) Blue layer segmented by CMSLEF



(d3) Blue layer segmented by Leyk's method

◀ **Fig. 11** Results of comparison experiment. The red rectangles show superiority of our method in connectivity and the blue rectangles indicate fewer interferential pixels in results of CMSLEF. For Leyk's method, we set $h_{crit}=0.95$, $d_{crit}=40$ and $c_{crit}=80$

4 The evaluation metric

At present, the existing evaluation metrics of segmentation for topographic map are mainly based on comparison to manually plotted geographic elements [7, 10, 27]. These approaches evaluate segmentation results with methods of exhaustion, which can provide an objective evaluation. In this paper, we use completeness, correctness and quality [10] to evaluate the segmentation results. They are defined as following.

- Completeness is the percentage of reference lines which lie within the buffer around the extracted lines. It can be described as formula (4). The optimum value for the completeness is 1.

$$\begin{aligned} \text{completeness} &= \frac{\text{length of matched reference lines}}{\text{length of reference lines}} \\ \text{completeness} &\in [0, 1] \end{aligned} \quad (4)$$

- Correctness is the percentage of extracted lines which lie within the buffer around the reference lines. It can be described as formula (5). The optimum value for the correctness is 1.

$$\begin{aligned} \text{correctness} &= \frac{\text{length of matched extraction lines}}{\text{length of extraction lines}} \\ \text{correctness} &\in [0, 1] \end{aligned} \quad (5)$$

- Quality is a more general measure of the final result combining completeness and correctness. It can be described as formula (6). The optimum value for the quality is 1.

$$\begin{aligned} \text{quality} &= \frac{\text{length of matched extraction lines}}{\text{length of extraction lines} + \text{length of unmatched reference lines}} \\ \text{quality} &\in [0, 1] \end{aligned} \quad (6)$$

The definitions of factors appear in these metrics are illustrated in Fig. 8. All the lines in Fig. 8 represent the lines after thinning process. The length of a line is the number of pixels in it. The buffer of reference lines are the manually extracted lines without thinning. And the buffer width of extracted lines is always 1 pixel in these evaluation metrics.

Table 1 Evaluation of results in Fig. 10

method	image label	completeness	correctness	quality
FCM based on pixels	b1	0.9872	0.9132	0.9025
	c1	0.9358	0.8679	0.8191
	d1	0.9562	0.6900	0.6689
	e1	0.8128	0.1728	0.1662
CMSLEF	b2	0.9908	0.9943	0.9852
	c2	0.9755	0.9757	0.9523
	d2	0.8975	0.9802	0.8816
	e2	0.9693	0.9244	0.8981
Leyk's method	b3	0.9633	0.8911	0.8618
	c3	0.9683	0.5924	0.5811
	d3	0.9338	0.9573	0.8965
	e3	0.8852	0.7940	0.7198

5 Experiments and analysis

In order to verify the validity of our proposed algorithm, three experiments are given in this section. Experiment 1 is used to illustrate the results of each procedure of our method CMSLEF. The other experiments are designed to compare the performances of different algorithms.

5.1 Intermediate and final results of CMSLEF

According to CMSLEF, the results of each experimental procedure are shown in Fig. 9. The original image with the size of 512×512 is segmented into 3 layers. We set the threshold $T=15$ in the areal elements removal method and $m=2$ in FCM for the CMSLEF. The number of clusters in FCM is manually assigned depend on how many geographic elements appear in the linear element map. Meanwhile, the cluster centers are initialized randomly. The original image, named Map0 is shown in Fig. 9a, and its linear element map after areal element removal, named Map1 is shown in Fig. 9b. Figure 9c is obtained by thinning Map1. It is the thinned linear element map, named Map2. The linear element map, named Map3, and the map of disconnected nodes, named Map4 are illustrated in Fig. 9d and e, respectively.

Table 2 Evaluation of results in Fig. 11

method	image label	completeness	correctness	quality
FCM based on pixels	b1	0.8906	0.3919	0.3739
	c1	0.9750	0.9620	0.9388
	d1	0.9382	0.8587	0.8128
CMSLEF	b2	0.7644	0.8544	0.6763
	c2	0.9417	0.9845	0.9279
	d2	0.8921	0.9232	0.8305
Leyk's method	b3	0.4751	0.9222	0.4568
	c3	0.9564	0.9132	0.8768
	d3	0.9933	0.5612	0.5591

Figure 9f shows the dilated linear element map, named Map5. Figure 9g to i shows the segmented layers, and the final results are shown in Fig. 9j to l.

From the final results we can see that the lines keep good continuity. In Fig. 9j, some brown pixels which caused by aliasing are not separated from the black layer they should belong to. In Fig. 9k, besides the false color, the merged disconnected nodes are also helpful to the continuity of river features. In Fig. 9l, mixed colors which caused by overlapping appear in this brown layer guarantee the integrity of contour lines. It can be seen that our algorithm can keep the continuity of linear elements under aliasing and false colors, which could hardly be achieved with other segmentation method based on pixels.

5.2 Comparison experiments

FCM algorithm has been widely used in image segmentation for the successfully introduction of fuzzification [2, 18, 30]. It is a partitioning method based on Picard iteration through necessary conditions for optimizing a weighted sum of objective functions. The conventional FCM method is employed to the comparison method which is based on pixels. The elementary

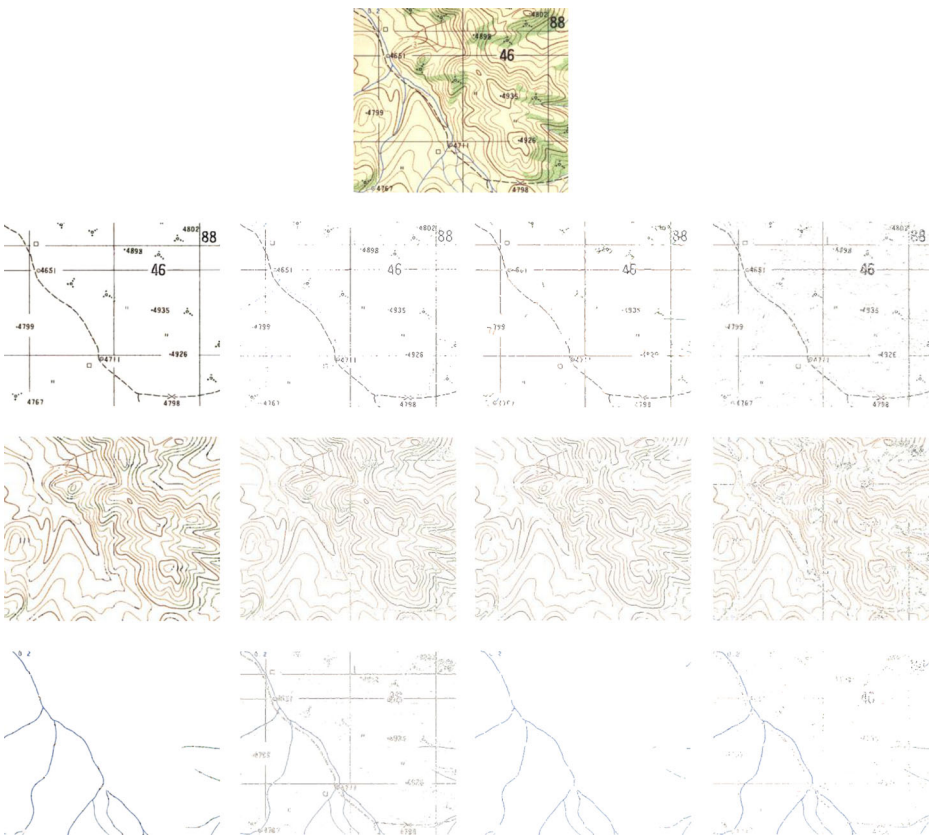


Fig. 12 Results of comparison experiment. The first row shows the original color map with the size of 460×393 . From the left column to the right one, they are referenced layers, results of FCM based on pixels, results of CMSLEF and results of Leyk's method. For Leyk's method, we set $h_{crit}=0.95$, $d_{crit}=50$ and $c_{crit}=100$

unit in calculation of comparison method is pixel and that of our method is the linear element. Thus in the CMSLEF, the size of data set is much smaller than that of comparison method, which lead to lower computation cost. We set $m=2$, manually assigned the number of clusters and randomly initialize the cluster centers for both methods and $T=15$ for CMSLEF in the following 5 comparison experiments. In addition, Leyk's method [16] is also employed to make comparisons with the CMSLEF. Leyk applied seeded region growing algorithm which based on homogeneity to segment color map into different layers. In his method, there are three important parameters which are homogeneity threshold h_{crit} , similar distance threshold d_{crit} and frequency threshold c_{crit} . The results shown in the following experiments of Leyk's method are achieved under the parameters which we adjust to appropriate ones.

Two maps with the size 512×512 are used to compare the performance of different methods. The experiment results with magnified regions are shown in Figs. 10 and 11. Figures 10a and 11a are the original maps and the first column shows the reference layers extracted manually from the original maps.

The experimental results show that the proposed algorithm achieves a better performance in information integrity, correctness and redundancy. As shown in

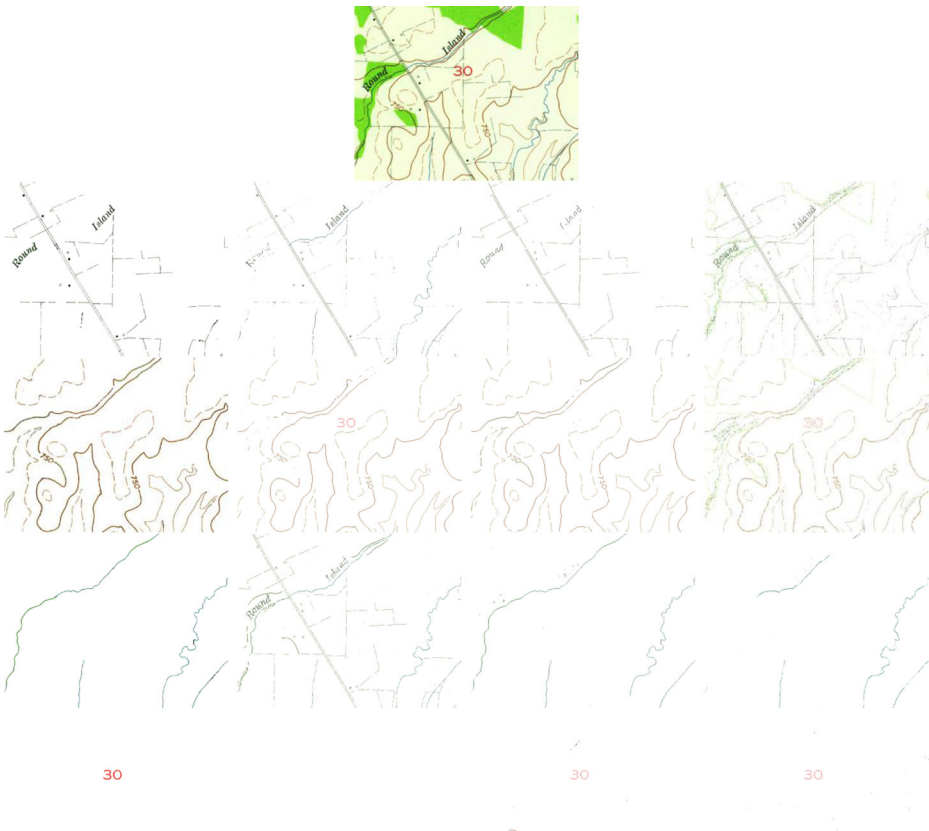


Fig. 13 Results of comparison experiment. The first row shows the original color map with the size 752×587 . From the left column to the right one, they are referenced layers, results of FCM based on pixels, results of CMSLEF and results of Leyk's method. For Leyk's method, we set $h_{crit}=0.95$, $d_{crit}=40$ and $c_{crit}=10$

Fig. 10c1 and c3, there are lots of breakages (red rectangles) in the contours, and there exists some pixels which should not belong to the contour (blue rectangle) in this figure. But these cases do not occur in Fig. 10c2. Similarly, these phenomena also can be seen in other figures. For the method based on pixels, the region information is not involved. It would make mistake in the segmentation results when there exists false colors and aliasing. In Leyk's method, the homogeneity in neighborhoods is employed. But in the region growing process, the inaccurate local information always leads to a succession of false segmentation. The color deviation not only causes gaps, for example, the gaps of contour lines shown in Fig. 10c1, but also introduce interferential pixels in other layers, which can be found from contour line points shown in Fig. 10d1 and e1. But CMSLEF can efficiently deal with these problems by regarding all pixels included in one geography element as a unit.

Furthermore, the evaluation in the following illustrates the advantage of the CMSLEF. We use the metrics introduced in section 4 to assess the experiment results. The evaluation results for Figs. 10 and 11 are shown in Tables 1 and 2, respectively. The image labels, e.g. b1, in Tables 1 and 2 are corresponding to the index of segmentation results in Figs. 10 and 11.

According to the tables shown above, the MSLEF reaches a higher completeness and correctness. The general metric quality further verifies a better performance of CMSLEF. It can be seen that except c2 of Table 2, the quality values of all layers obtained by CMSLEF are larger than those of other comparisons. The reason of c1 in Table 2 gets a larger quality value is

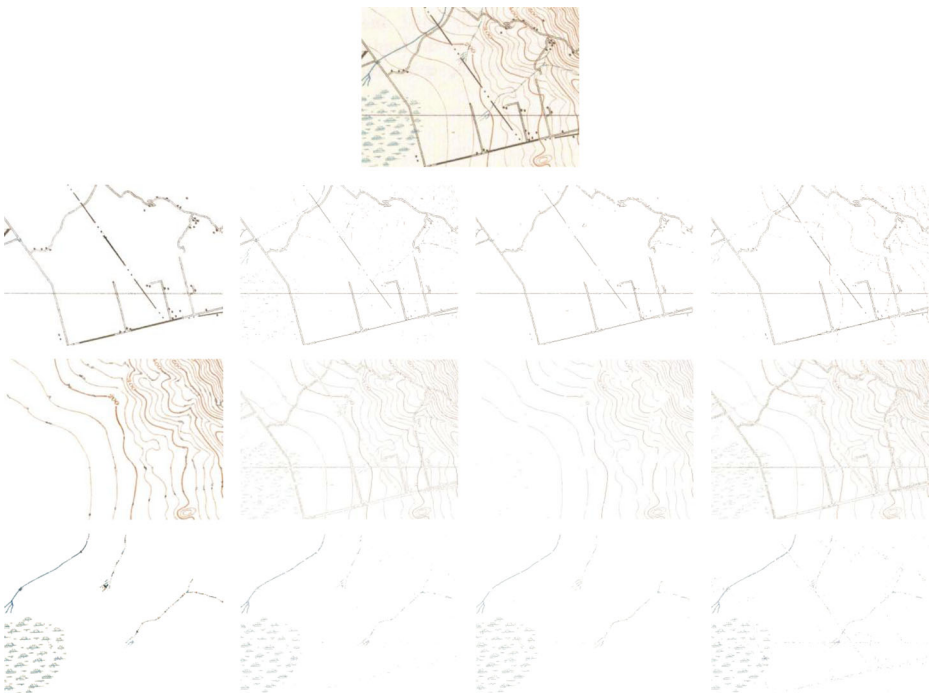


Fig. 14 Results of comparison experiment. The first row shows the original color map with the size 730×536 . From the left column to the right one, they are referenced layers, results of FCM based on pixels, results of CMSLEF and results of Leyk's method. For Leyk's method, we set $h_{crit}=0.95$, $d_{crit}=15$ and $c_{crit}=10$

Table 3 Quality of segmented layers in Figs. 12, 13 and 14

	FCM based on pixels	CMSLEF	Leyk's method
Fig. 12	0.6947	0.7881	0.6786
	0.8810	0.8935	0.7372
	0.2554	0.8367	0.5819
Fig. 13	0.4737	0.7651	0.3734
	0.8601	0.8931	0.5762
	0.2742	0.9059	0.4604
	—	0.6540	0.7665
Fig. 14	0.7858	0.9027	0.7558
	0.5298	0.7693	0.5203
	0.6973	0.7977	0.6238

not due to its high completeness and correctness. Actually, it is because that there are lots of small circles (as shown in Fig. 11c1) in the lines after thinning, which are caused by the inaccuracy segmentation. And these circles enlarge both the length of matched extracted lines and the length of matched reference lines. As a result, the value of its quality has become larger. In conclusion, from the tables it can be seen that our proposed method achieves a better performance in both completeness and correctness.

In order to further prove the good performance of CMSLEF, three another comparison experiments are shown in Figs. 12, 13, 14. The evaluations of these experiment results are shown in Table 3.

It is worth noting that in Fig. 13, the last image in the second column is white. That is because, the method FCM based on pixels cannot separate the red '30' from the brown layer successfully. It could be caused by the fact that the size of the red data is too small to be regarded as one cluster during clustering. From the comparison experiments shown above, CMSLEF performs better in both completeness and correctness intuitively. The quality metric shown in Table 3 verifies the better performance of CMSLEF. In this table, the position of a unit corresponds to the position in its belonged figure. For example, the white image mentioned previously in Fig. 13 lies on the fourth row of the results obtained by pixels based FCM. Thus in Table 3, its quality value, which is null, lies on the fourth row of the first column in the sub-table in Fig. 13.

From Table 3, except the red layer in Fig. 13, all the CMSLEF results achieve a higher quality. This means the CMSLEF perform better in preserving both completeness and correctness of the segmented layers. Meanwhile, in all of these five comparison experiments, the energy density difference threshold T is set as 15 and the fuzzy exponent m is set as 2. Therefore, the results are not sensitive to the parameters in the proposed method. In order to verify the robustness of parameter T , the quality evaluations of different results of Fig. 13

Table 4 Quality of segmented layers of Fig. 13 in different T

$T=5$	$T=10$	$T=15$	$T=20$	$T=25$	$T=30$	$T=35$
0.5224	0.7602	0.7651	0.7651	0.7563	0.7563	0.7241
0.5116	0.8843	0.8931	0.8931	0.8903	0.8903	0.8341
0.2340	0.8878	0.9059	0.9059	0.9034	0.9034	0.7748
0.0054	0.6540	0.6540	0.6540	0.7042	0.7042	0.4983

which achieved in various T are shown in Table 4. It can be seen that the quality almost stay the same in a large range of T (from 10 to 30). Moreover, the elementary unit in calculation of our method is linear element, which means the size of data set is much smaller than that of FCM based on pixels, which leads to a lower computation cost.

6 Conclusion

An algorithm named CMSLEF for color map segmentation is proposed in this paper. In our method, linear elements are regarded as the elementary units in segmentation for solving the problems of color deviation interference and the discontinuity of segmentation results in conventional segmentation methods. The experimental results show that the segmented layers can be obtained more accurately based on the proposed algorithm than that based on other methods. Meanwhile, CMSLEF is a robust and fast algorithm due to the insensitive parameters and small data set in calculation.

Acknowledgments The work was jointly supported by the National Natural Science Foundations of China under grant No. 61272280, 41271447, 61272195 and 61472302, the Program for New Century Excellent Talents in University (NCET-12-0919), the Fundamental Research Funds for the Central Universities under grant No. K5051203020, K5051303016, K5051303018, BDY081422, and K50513100006, the Creative Project of the Science and Technology State of xi'an under grant No. CXY1341(6), The State Key Laboratory of Geo-information Engineering under grant No. SKLGIIE2014-M-4-4.

References

1. Ahmed MN, Yamany SM, Mohamed N, Farag AA, Moriarty T (2002) A modified fuzzy c-means algorithm for bias field estimation and segmentation of MRI data. *IEEE Trans Med Imaging* 21(3):193–199
2. Biosca JM, Lerma JL (2008) Unsupervised robust planar segmentation of terrestrial laser scanner point clouds based on fuzzy clustering methods. *ISPRS J Photogramm Remote Sens* 63(1):84–98
3. Cai W, Chen S, Zhang D (2007) Fast and robust fuzzy c-means clustering algorithms incorporating local information for image segmentation. *Pattern Recogn* 40(3):825–838
4. Campadelli P, Medici D, Schettini R (1997) Color image segmentation using Hopfield networks. *Image Vis Comput* 15(3):161–166
5. Celenk M (1990) A color clustering technique for image segmentation. *Comput Vision, Graphics, Image Process* 52(2):145–170
6. Chen H, Tang XA, Wang CH, Gan Z (2010) Object oriented segmentation of scanned topographical maps. *J Image Graph* 9:020
7. Chen Y, Wang R, Qian J (2006) Extracting contour lines from common-conditioned topographic maps. *IEEE Trans Geosci Remote Sens* 44(4):1048–1057
8. Gonzalez RC, Woods RE (2007) *Digital image processing*. Publishing House of Electronics Industry, Beijing, pp 423–439
9. Hathaway RJ, Bezdek JC (2001) Fuzzy c-means clustering of incomplete data. *IEEE Trans Syst Man Cybern B: Cybern* 31(5):735–744
10. Heipke C, Mayer H, Wiedemann C, Jamet O (1997) Evaluation of automatic road extraction. *Int Arch Photogramm Remote Sens* 32:151–160
11. Huang CL (1992) Parallel image segmentation using modified Hopfield model. *Pattern Recogn Lett* 13(5): 345–353
12. Khotanadz A, Zink E (2003) Contour line and geographic feature extraction from USGS color topographical paper maps. *IEEE Trans Pattern Anal Mach Intell* 25(1):18–31

13. Kuntimad G, Ranganath HS (1999) Perfect image segmentation using pulse coupled neural networks. *IEEE Trans Neural Netw* 10(3):591–598
14. Kurugollu F, Sankur B, Harmanci AE (2001) Color image segmentation using histogram multithresholding and fusion. *Image Vis Comput* 19(13):915–928
15. Leyk, S (2010) Segmentation of colour layers in historical maps based on hierarchical colour sampling. In *Graphics Recognition. Achievements, Challenges, and Evolution*. Springer Berlin Heidelberg, pp 231–241
16. Leyk S, Boesch R (2010) Colors of the past: color image segmentation in historical topographic maps based on homogeneity. *GeoInformatica* 14(1):1–21
17. Lim WQ (2010) The discrete shearlet transform: a new directional transform and compactly supported shearlet frames. *IEEE Trans Image Process* 19(5):1166–1180
18. Lim YW, Lee SU (1990) On the color image segmentation algorithm based on the thresholding and the fuzzy c-means techniques. *Pattern Recogn* 23(9):935–952
19. Miao Q, Xu P, Liu T, Yang Y, Zhang J, Li W (2013) Linear feature separation from topographic maps using energy density and the shear transform. *IEEE Trans Image Process* 22(4):1548–1558
20. Ohlander R, Price K, Reddy DR (1978) Picture segmentation using a recursive region splitting method. *Comput Graph Image Process* 8(3):313–333
21. Ong SH, Yeo NC, Lee KH, Venkatesh YV, Cao DM (2002) Segmentation of color images using a two-stage self-organizing network. *Image and. Vision Comput* 20(4):279–289
22. Otsu N (1975) A threshold selection method from gray-level histograms. *Automatica* 11(285–296):23–27
23. Stewart RD, Fermin I, Opper M (2002) Region growing with pulse-coupled neural networks: an alternative to seeded region growing. *IEEE Trans Neural Netw* 13(6):1557–1562
24. Sun JG, Liu J, Zhao LY (2008) Clustering algorithms research. *J Software* 19(1):48–61
25. Tombe K (1995) Graphics recognition—general context and challenges. *Pattern Recogn Lett* 16(9):883–891
26. Wei S, Hong Q, Hou M (2011) Automatic image segmentation based on PCNN with adaptive threshold time constant. *Neurocomputing* 74(9):1485–1491
27. Wiedemann C, Heipke C, Mayer H, Jamet O (1998) Empirical evaluation of automatically extracted road axes. *Empirical Evaluation Techniques in Computer Vision* 172–187
28. Xin D, Zhou X, Zheng H (2006) Contour line extraction from paper-based topographic maps. *J Inf Comput Sci* 1(5):275–283
29. Xu R, Wunsch D (2005) Survey of clustering algorithms. *IEEE Trans Neural Netw* 16(3):645–678
30. Zheng H, Zhou X, Wang J (2003) Research and implementation of automatic color segmentation algorithm for scanned color maps. *J Comput Aided Des Comput Graph* 1:003
31. Zhuang H, Low KS, Yau WY (2012) Multichannel pulse-coupled-neural-network-based color image segmentation for object detection. *IEEE Trans Ind Electron* 59(8):3299–3308



Tiange Liu He is currently pursuing the Doctor degree in Computer Application Technology at xidian University in China. His main research interests include: the Intelligent image processing.



Qiguang Miao Professor at School of Computer Science and Technology, Xidian University. His research interests include: the Intelligent image processing, and multiscale geometric representations for image.



Pengfei Xu He is currently pursuing the Doctor degree in Computer Application Technology at xidian University in China. His main research interests include: the Intelligent image processing.



Jianfeng Song Lecturer at School of Computer Science and Technology, Xidian University. His research interests include: the system security.



Yining Quan Associate professor at School of Computer Science and Technology, Xidian University. His research interests include: the network computing and network security.